

Strain effects on excitonic transitions in GaN: Deformation potentials

W. Shan, R. J. Hauenstein, A. J. Fischer, and J. J. Song

Center for Laser Research and Department of Physics, Oklahoma State University, Stillwater, Oklahoma 74078

W. G. Perry, M. D. Bremser, and R. F. Davis

Department of Materials Science and Engineering, North Carolina State University, Raleigh, North Carolina 27695

B. Goldenberg

Honeywell Technology Center, Plymouth, Minnesota 55441

(Received 11 July 1996)

We present the results of experimental studies of the strain effects on the excitonic transitions in GaN epitaxial layers on sapphire and SiC substrates, with the emphasis on the determination of deformation potentials for wurtzite GaN. Photoluminescence and reflectance spectroscopies were performed to measure the energy positions of exciton transitions and x-ray-diffraction measurements were conducted to examine the lattice parameters of GaN epitaxial layers grown on different substrates. Residual strain induced by the mismatch of lattice constants and thermal expansion between GaN epitaxial layers and substrates was found to have a strong influence in determining the energies of excitonic transitions. The overall effects of the strain generated in GaN is compressive for GaN grown on sapphire and tensile for GaN on SiC substrate. The uniaxial and hydrostatic deformation potentials of wurtzite GaN were derived from the experimental results. Our results yield the uniaxial deformation potentials $b_1 \approx -5.3$ eV and $b_2 \approx 2.7$ eV, as well as the hydrostatic components $a_1 \approx -6.5$ eV and $a_2 \approx -11.8$ eV. [S0163-1829(96)06843-9]

GaN-based III-V nitride semiconductors currently attract extensive attention for their potential device applications.¹⁻³ It is known that GaN has a wurtzite structure in natural form, and has a wide direct band gap of ~ 3.42 eV at 300 K, which provides efficient radiative recombination. The wavelength of radiation from GaN-based materials can be tuned over a wide range from visible to ultraviolet by alloying or forming heterostructures, such as quantum wells, with other nitrides (AlN and InN). These merits make III-V nitrides very attractive to short-wavelength optical applications such as light emitters and detectors operating in the blue and ultraviolet wavelength range. The outstanding thermal and chemical stability of the wide-band-gap nitrides also allows GaN-based electronic and optoelectronic devices to operate at high temperatures and in hostile environments.

Great efforts have recently been devoted to the preparation of high-quality GaN crystals and epitaxial films, the characterization of GaN crystals and films, and the development of devices using GaN-based materials. In the course of these studies, a number of investigations on the optical properties of GaN have revealed that there is a relatively large difference in the reported values of observed energy positions of excitonic transitions in GaN.⁴⁻¹¹ It is found that the energy positions vary from sample to sample depending on the epitaxial layer thickness, growth techniques and substrate materials. Such discrepancy has been attributed to the effects of residual strain in the epilayers due to the mismatch of lattice parameters and coefficients of thermal expansion between GaN and the substrate materials.^{8,11,12} In this report, we present the results of experimental studies of the strain effects on the excitonic transitions in GaN epitaxial layers on sapphire and SiC substrates. Photoluminescence and reflectance spectroscopies were performed to examine the effects of strain on the exciton transitions in the GaN epitaxial materials on sapphire and SiC substrates. X-ray-diffraction mea-

surements were conducted to measure the lattice parameters of GaN epitaxial layers grown on different substrates. The residual strain built in GaN epitaxial films induced by the mismatch of lattice constants and thermal expansion between GaN epitaxial layers and substrates was found to play an important role in determining the energies of excitonic transitions. The overall effects of the strain generated in GaN is compressive for GaN grown on sapphire and tensile for GaN on SiC substrate. The uniaxial and hydrostatic deformation potentials were derived from the experimental results.

The GaN samples used in this work were nominally undoped single-crystal films grown by metalorganic chemical vapor deposition on (0001) 6H-SiC or basal-plane sapphire substrates. AlN buffer layers were deposited on the substrates at about 775 °C before the growth of the GaN epilayers.¹³ Photoluminescence (PL) measurements were conducted with either a cw HeCd laser (325 nm) or a frequency-doubled Ar⁺ laser (244 nm) as the excitation source and a 1-M double-grating monochromator connected to a photon-counting system. For reflectance measurements, the quasimonochromatic light dispersed by a $\frac{1}{2}$ -M monochromator from a xenon lamp was focused on samples, and the reflectance signals were detected using a lock-in amplification system. To determine the lattice parameters of GaN epitaxial films, four-crystal x-ray rocking curves were measured. Absolute lattice parameter measurements were performed in the triple-axis mode of a Philips high-resolution diffractometer with four-bounce Ge (220) incident beam optics and three-bounce Ge (220) diffracted beam optics. The resolution limit of this configuration is ~ 10 arc sec. The high resolution of the triple-bounce analyzer crystal and the steps taken to eliminate inaccuracies due to the 2θ zero error as well as sample centering account for the limit. The data were collected using 2θ - ω scans, with corrections made for refraction. The accuracy of lattice parameters measured

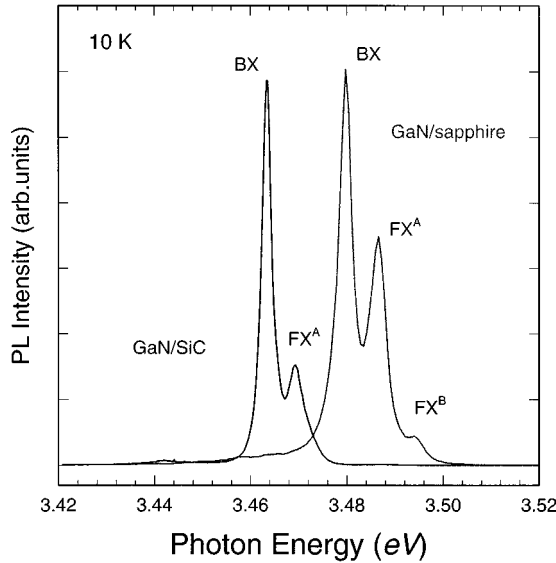


FIG. 1. Near-band-edge exciton luminescence spectra taken from a 3.7- μm GaN epilayer on SiC and a 4.2- μm GaN epilayer on sapphire at 10 K.

using this system is predicted to be better than 0.0002 \AA . The high resolution of the triple-bounce analyzer crystal and the steps taken to eliminate inaccuracies due to the 2θ zero error as well as sample centering account for this. The lattice parameter c was measured using the (002) reflection and a was measured using both the (002) and (015) reflections.

The GaN-based samples studied in this work all exhibit strong near-band-edge exciton luminescence. Results of PL measurements from a 3.7- μm GaN epilayer on SiC and a 4.2- μm sample with sapphire substrate are shown in Fig. 1. The intensity of the strongest emission line marked by BX in Fig. 1 was found to decrease much faster than that labeled FX as the temperature increased. It became hardly resolvable at temperatures higher than 100 K. Such variations of the luminescence intensity as a function of temperature indicate that the emission line can be attributed to the radiative recombination of excitons bound to neutral donors.⁷ The second strongest luminescence structure, together with the weak emission feature on the higher-energy side, are a radiative recombination of the intrinsic free exciton. As clearly illustrated by the figure, the values of PL transition energies obtained here from GaN on an SiC substrate are lower than those from GaN on sapphire. The energy positions of the BX peak and FX peak are 3.4634 and 3.4693 eV, respectively, for the GaN/SiC sample, and 3.4790 and 3.4845 eV, respectively, for the GaN/sapphire sample. Figure 2 shows the comparison of the reflectance spectra taken from the same two samples at 10 K. Three exciton resonances associated with the transitions referred to as the A , B , and C exciton transitions⁴⁻⁷ between the bottom of the conduction band (Γ_7^c) and three topmost valence-band edges ($\Gamma_9^v + \Gamma_7^v + \Gamma_7^v$) are indicated by vertical arrows. The energy positions of these transitions are 3.470, 3.474, and 3.491 eV, respectively, for the GaN/SiC sample while the corresponding values, 3.485, 3.493, and 3.518 eV, were obtained for GaN on sapphire. Such systematically observed differences in exciton transition energies have been attributed to the effects of residual strain in the epilayers due to the mismatch of lattice

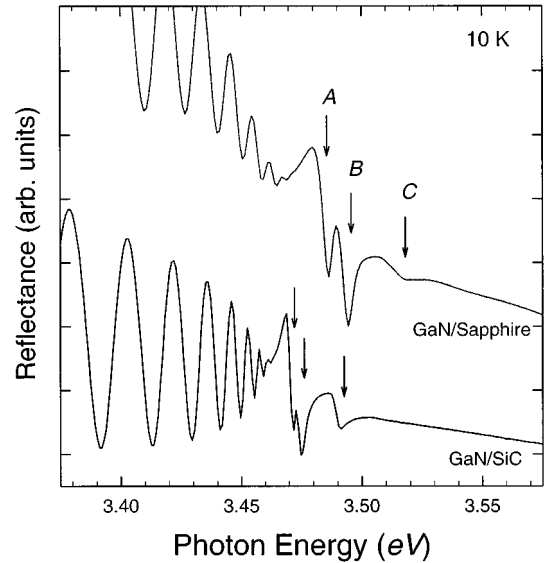


FIG. 2. Reflectance spectra of the exciton transition region of the MOCVD GaN/SiC and GaN/sapphire samples at 10 K. The oscillatory structures at lower energy are interference effects caused by the heterointerface.

parameters and coefficients of thermal expansion between GaN and the substrate materials.^{8,11,12}

Because of the inevitable occurrence of strain relaxation by the formation of a large density of dislocations, it is generally difficult to separate the strain effects caused by lattice-parameter mismatch from the ones involving thermal-expansion mismatch so as to exactly determine their influences on the optical properties of GaN epitaxial layers. However, by comparing the observed exciton transition energies in GaN epilayers deposited on sapphire and SiC to the values (3.4751, 3.4815, and 3.503 eV) obtained from virtually strain-free bulk GaN reported in Ref. 6, one can infer that the overall effects of residual strain generated in GaN on sapphire is compressive, which results in an increased band gap, while that induced in GaN on SiC is tensile, which leads to a decrease in measured exciton transition energies. This was further confirmed by x-ray rocking curve measurements. The lattice parameters were determined to be $a=3.1848 \text{ \AA}$ and $c=5.1879 \text{ \AA}$ for the 4.2- μm GaN on sapphire and $a=3.1900 \text{ \AA}$ and $c=5.1840 \text{ \AA}$ for the 3.7- μm GaN on SiC, compared to the lattice parameters of $a=3.1891 \text{ \AA}$ and $c=5.1855 \text{ \AA}$ for strain-free GaN.¹⁴ Therefore, the results presented here lead to the conclusion that residual strain induced by thermal-expansion mismatch in GaN-based epitaxial layers has the prevailing influence on the energy variations of exciton transitions, since lattice-mismatch induced strain is of the opposite sign and hence would have the opposite effect on the variation of GaN band gap from that observed.

The observed strain shifts in excitonic transition energies permit a direct estimate of the deformation potentials, including both hydrostatic and uniaxial components for wurtzite GaN. The strain Hamiltonian of a material having a wurtzite structure is given by Pikus.¹⁵ Under the assumption of a strain-independent and isotropic spin-orbit interaction, the energies of the three free excitons A , B , and C can be described as^{16,17}

$$E_A = E_A(0) + \mathbf{a}_1 \epsilon_{zz} + \mathbf{a}_2 (\epsilon_{xx} + \epsilon_{yy}) + \mathbf{b}_1 \epsilon_{zz} + \mathbf{b}_2 (\epsilon_{xx} + \epsilon_{yy}), \quad (1)$$

$$E_B = E_B(0) + \mathbf{a}_1 \epsilon_{zz} + \mathbf{a}_2 (\epsilon_{xx} + \epsilon_{yy}) + \Delta_+ [\mathbf{b}_1 \epsilon_{zz} + \mathbf{b}_2 (\epsilon_{xx} + \epsilon_{yy})], \quad (2)$$

$$E_C = E_C(0) + \mathbf{a}_1 \epsilon_{zz} + \mathbf{a}_2 (\epsilon_{xx} + \epsilon_{yy}) + \Delta_- [\mathbf{b}_1 \epsilon_{zz} + \mathbf{b}_2 (\epsilon_{xx} + \epsilon_{yy})], \quad (3)$$

where $E_i(0)$ represents strain-free exciton transition energy, \mathbf{a} and \mathbf{b} are deformation potentials, and the ϵ_{ii} are components of the strain tensor for the GaN film. Since the energy variation given in Eqs. (1)–(3) by \mathbf{a}_1 and \mathbf{a}_2 is analogous to the hydrostatic shift of a cubic semiconductor, \mathbf{a}_1 and \mathbf{a}_2 are combined hydrostatic deformation potentials for transitions between the conduction and the valence bands, while \mathbf{b}_1 and \mathbf{b}_2 are uniaxial deformation potentials characterizing the further splitting of the three topmost valence-band edges for tension or compression along and perpendicular to (0001), respectively. Since the growth direction of our epilayers is the z axis, the strain components are described by

$$\epsilon_{xx} = \epsilon_{yy} = \epsilon_{\parallel} = (a_s - a_0)/a_0, \quad \epsilon_{zz} = \epsilon_{\perp} = (c_s - c_0)/c_0, \quad (4)$$

where a_0 and c_0 are lattice parameters for strain-free bulk GaN, and a_s and c_s are those for the strained GaN epilayer. Under biaxial-stress conditions, the components of ϵ_{xx} , ϵ_{yy} , and ϵ_{zz} are related through the elastic stiffness coefficients as $\epsilon_{\perp} = -2C_{13}/C_{33}\epsilon_{\parallel}$. The coefficients Δ_{\pm} represent the mixing of valence-band orbital states by the spin-orbit interaction and are given by^{16,17}

$$\Delta_{\pm} = \frac{1}{2} \{ 1 \pm [1 + 8(\Delta_3/(\Delta_1 - \Delta_2))^2]^{-1/2} \}, \quad (5)$$

where Δ_1 is the crystal-field splitting of the Γ_9 and Γ_7 orbital states, Δ_2 and Δ_3 are parameters which describe the spin-orbit coupling. In principle, one has to know the values of these three band-structure parameters, in addition to the deformation potentials to predict strain shifts from Eqs. (1)–(3) above. This approach is complicated by the lack of consistent numerical values for the parameters, Δ_i .^{4,8,10,18–20} Fortunately, Eqs. (2) and (3) only require a knowledge of the ratio, $\gamma = \Delta_3/(\Delta_1 - \Delta_2)$, rather than the individual numerical values for these parameters. By plotting the observed excitonic transition energies against the residual strain in Fig. 3, we were able to obtain a value of ~ 0.531 for γ from the slopes of the solid lines in the figure.

The observed shifts in excitonic transition energies relative to the values of strain-free GaN (Refs. 5, 6, and 8) result from an overall effect of strain on the band gap which includes contributions from both hydrostatic and uniaxial components of the stress. To determine the respective values for the uniaxial and hydrostatic potentials of wurtzite GaN, one has to separate their contributions to the energy variations in observed exciton transition energies under strain compared to the strain-free case. By taking the differences between the experimentally obtained values of each individual excitonic transition according to Eqs. (1)–(3), the uniaxial component of strain-induced energy shift of the conduction-band edge relative to the valence-band edges can be readily separated from the total energy shift. With linear fits to the whole set of data listed in Table I using the least-square fitting, our results yield the relationship of the uniaxial deformation potentials \mathbf{b}_1 and \mathbf{b}_2 :

$$\mathbf{b}_1 - C_{33}/C_{13}\mathbf{b}_2 = -15.2 \text{ eV}. \quad (6)$$

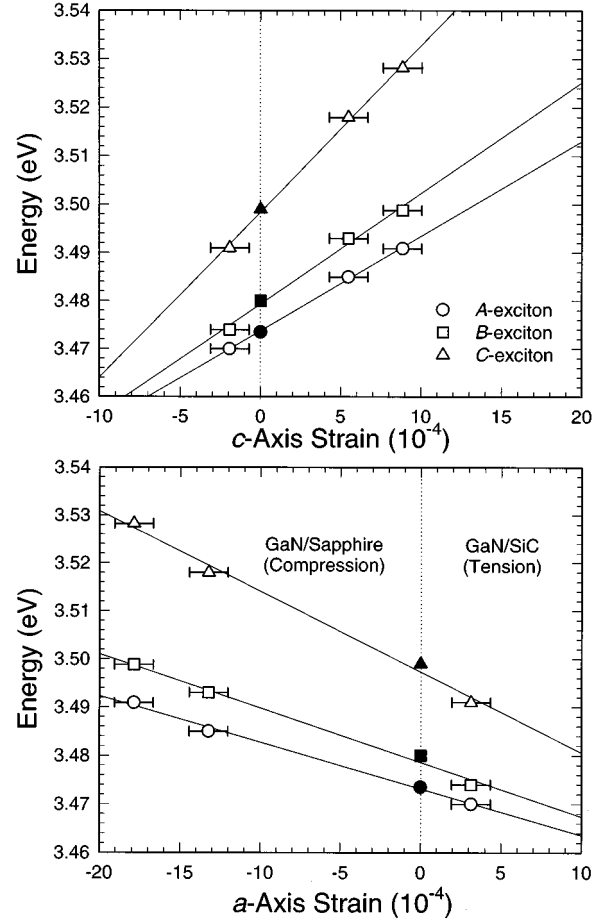


FIG. 3. The measured excitonic transition energies from GaN samples used in this work as a function of relative in-plane (biaxial) strain (lower portion) as well as the relative strain along the c axis (upper portion). The exciton transition energies of strain-free GaN were included in the figure for reference. The solid lines are the best linear fits to the experimental data.

A similar approach allows us to relate the combined hydrostatic deformation potentials \mathbf{a}_1 and \mathbf{a}_2 to each other as

$$\mathbf{a}_1 - C_{33}/C_{13}\mathbf{a}_2 = 37.9 \text{ eV}, \quad (7)$$

by subtracting the contribution of uniaxial component of strain from the total-energy shift induced by strain. Based on the facts that the strain-caused total-energy shift relative to the excitonic transition energy is very small and the elastic properties of GaN are of quasicubic nature ($C_{11} \approx C_{33}$),^{21,22} we found that it is appropriate to estimate the numerical val-

TABLE I. Values of measured excitonic transition energies and built-in residual strain for GaN on SiC and sapphire, together with those for strain-free bulk GaN.

	GaN/sapphire		GaN/bulk	GaN/SiC
Thickness (μm)	4.2	7.2	>100 ^a	3.7
A exciton (eV)	3.485	3.491	3.4735 ^a	3.470
B exciton (eV)	3.493	3.499	3.4800 ^a	3.474
C exciton (eV)	3.518	3.528	3.4993 ^a	3.491
ϵ_{\parallel} (10^{-4})	-13.2	-17.9	0	3.1
ϵ_{\perp} (10^{-4})	5.5	8.9	0	-1.9

^aReferences 5, 6, and 8.

ues, within the range of linear dependence on strain, for the uniaxial and hydrostatic deformation potentials using quasicycubic approximation²³ with $\mathbf{b}_1 \approx -2\mathbf{b}_2$, and $\mathbf{a}_1 - \mathbf{a}_2 \approx 2\mathbf{b}_2$. The uniaxial deformation potentials are readily estimated to be $\mathbf{b}_1 \approx -5.3$ eV and $\mathbf{b}_2 \approx 2.7$ eV, using the values $C_{13} = 106$ and $C_{33} = 398$ GPa.²² The uncertainty of the above estimates is $\sim 15\%$, originating primarily from experimental error in the precise determination of lattice parameters. Our numerical values are comparable to the results reported for the materials with similar crystal structures such as CdS and ZnO,^{17,24} as well as recently reported values for GaN.^{8,20} Additionally, the numerical estimates for \mathbf{a}_1 and \mathbf{a}_2 are readily determined, once the values for \mathbf{b}_1 and \mathbf{b}_2 are known. Our results yield $\mathbf{a}_1 \approx -6.5$ eV and $\mathbf{a}_2 \approx -11.8$ eV.

It should be pointed out that the results of deformation potentials calculated using Eqs. (6) and (7) are dependent on the numerical values of the elastic stiffness constants C_{13} and C_{33} , especially for the hydrostatic parameters. For instance, the respective values of \mathbf{a}_1 and \mathbf{a}_2 could be as large as >20 eV if values, $C_{13} = 158$ and $C_{33} = 267$ GPa,²¹ are used. Fortunately, we were able to make a comparison of the estimated deformation potentials, obtained using variously reported values for C_{13} and C_{33} , with our previous work, in which a value for the “effective hydrostatic deformation potential” \mathbf{a} of -9.2 eV for the Γ band gap of GaN was determined.²⁵ The value of \mathbf{a} was determined by direct application of hydrostatic pressure. The reason for the term, *effective* hydrostatic deformation potential is that, strictly speaking, it is the stress, but (for the wurtzite structure) not the strain, that is isotropic, so that the terms involving \mathbf{b}_1 and \mathbf{b}_2 will contribute slightly in Eqs. (1)–(3). Thus, we regard the results of $\mathbf{b}_1 \approx -5.3$ eV and $\mathbf{b}_2 \approx 2.7$ eV as well as $\mathbf{a}_1 \approx -6.5$ eV and $\mathbf{a}_2 \approx -11.8$ eV as consistent and more accurate estimates, given the assumptions described above. Fi-

nally, we note that these in principle should represent an upper limit for the deformation potentials since they were evaluated by using the value of the lattice parameters measured at room temperature to fit optical data obtained at 10 K. The built-in residual strain is generally expected to increase with decreasing temperature due to the difference of thermal expansion coefficients between GaN epilayers and substrate materials.

In conclusion, we have studied the effects of residual strain in GaN epitaxial films using spectroscopic methods combined with x-ray-diffraction measurements, with the emphasis on determination of deformation potentials. Strong, sharp spectral structures associated with exciton transitions in GaN epitaxial layers grown on sapphire and 6H-SiC substrates by metal-organic chemical-vapor deposition (MOCVD) were observed in photoluminescence and reflectance spectra. The observation of exciton transitions with *lower* energies in GaN grown on SiC, and with *higher* energies for the same transitions for GaN grown on sapphire, in comparison to those obtained from strain-free bulk GaN, suggests that residual strain in GaN epilayers resulting from lattice-parameter and thermal-expansion mismatch plays an important role in determining the precise exciton transition energies. X-ray-diffraction measurements were performed to determine the variations in the lattice parameters of GaN epilayers on SiC and sapphire, respectively. Our results clearly indicate that GaN epilayers grown on SiC exhibit basal tensile strain, while those on sapphire substrates are under biaxial compression. Based on these results, the values of the four principal deformation potentials of wurtzite GaN have been determined.

This work at OSU was supported by AFOSR, DARPA, ONR, and ARO. The work at NCSU was supported by ONR under Contract No. N00014-92-J-1477.

-
- ¹J. I. Pankove, Mater. Res. Soc. Symp. Proc. **162**, 515 (1990), and references therein.
- ²S. Strite and H. Morkoç, J. Vac. Sci. Technol. B **10**, 1237 (1992), and references therein.
- ³H. Morkoç, S. Strite, G. B. Gao, M. E. Lin, B. Sverdlov, and M. Burns, J. Appl. Phys. **76**, 1363 (1994).
- ⁴R. Dingle and M. Ilegeme, Solid State Commun. **9**, 175 (1971).
- ⁵R. Dingle, D. D. Sell, S. E. Stokowski, and M. Illegems, Phys. Rev. B **4**, 1211 (1971).
- ⁶B. Monemar, Phys. Rev. B **10**, 676 (1974).
- ⁷W. Shan, T. J. Schmidt, X. H. Yang, S. J. Hwang, J. J. Song, and B. Goldenberg, Appl. Phys. Lett. **66**, 985 (1995).
- ⁸B. Gil, O. Briot, and R.-L. Aulombard, Phys. Rev. B **52**, R17 028 (1995).
- ⁹M. Smith, G. D. Chen, J. Y. Lin, H. X. Jiang, M. Asif Khan, C. J. Sun, Q. Chen, and J. W. Yang, J. Appl. Phys. **76**, 7001 (1996).
- ¹⁰G. D. Chen, M. Smith, J. Y. Lin, H. X. Jiang, S. H. Wei, M. Asif Kahn, and C. J. Sun, Appl. Phys. Lett. **68**, 2784 (1996).
- ¹¹W. Shan, A. J. Fischer, J. J. Song, G. E. Bulman, H. S. Kong, M. T. Leonard, W. G. Perry, M. D. Bremser, and R. F. Davis, Appl. Phys. Lett. **69**, 740 (1996).
- ¹²W. Rieger, T. Metzger, H. Angerer, R. Dimitrov, O. Ambacher, and M. Stutzmann, Appl. Phys. Lett. **68**, 970 (1996).
- ¹³T. W. Weeks, Jr., M. D. Bremser, K. S. Ailey, E. Carlson, W. G. Perry, and R. F. Davis, Appl. Phys. Lett. **67**, 401 (1995).
- ¹⁴C. M. Balkas, C. Basceri, and R. F. Davis, Powder Diffraction **10**, 266 (1995).
- ¹⁵G. Pikus, Zh. Eksp. Teor. Fiz. **41**, 1507 (1961) [Sov. Phys. JETP **14**, 1075 (1962)].
- ¹⁶V. B. Sandomirskii, Sov. Phys. Solid State **6**, 261 (1964).
- ¹⁷A. Gavini and M. Cardona, Phys. Rev. B **1**, 672 (1970).
- ¹⁸M. Suzuki, T. Uenoyama, and A. Yanase, Phys. Rev. B **52**, 8132 (1995).
- ¹⁹Yu. M. Sirenko, J. B. Jeon, K. W. Kim, M. A. Littlejohn, and M. A. Strocio, Phys. Rev. B **53**, 1997 (1996).
- ²⁰S. Chichibu, A. Shikanai, T. Azuhata, T. Sota, A. Kuramata, K. Horino, and S. Nakamura, Appl. Phys. Lett. **68**, 3766 (1996).
- ²¹V. A. Savastenko and A. U. Sheleg, Phys. Status Solidi A **48**, K135 (1978).
- ²²A. Polian, M. Grimsditch, and I. Grzegory, J. Appl. Phys. **79**, 3343 (1996).
- ²³G. L. Bir and G. E. Pikus, in *Symmetry and Strain-induced Effects in Semiconductors* (Wiley, New York, 1974), Chap. V.
- ²⁴D. W. Langer, R. N. Euwema, K. Era, and T. Koda, Phys. Rev. B **2**, 4005 (1970).
- ²⁵W. Shan, T. J. Schmidt, R. J. Hauenstein, J. J. Song, and B. Goldenberg, Appl. Phys. Lett. **66**, 3492 (1995).